

C. Kvarnström · A. Petr · P. Damlin · T. Lindfors
A. Ivaska · L. Dunsch

Raman and FTIR spectroscopic characterization of electrochemically synthesized poly(triphenylamine), PTPA

Received: 26 October 2001 / Accepted: 11 February 2002 / Published online: 22 March 2002
© Springer-Verlag 2002

Abstract Triphenylamine was electrochemically polymerized in a mixture of toluene and acetonitrile with different electrolyte salts. The poly(triphenylamine) (PTPA) films are insoluble in polar solvents and show high stability and no degradation or loss in electrochemical properties when stored in a laboratory atmosphere. The PTPA films were characterized in situ by FTIR external reflection spectroscopy and by Raman spectroscopy.

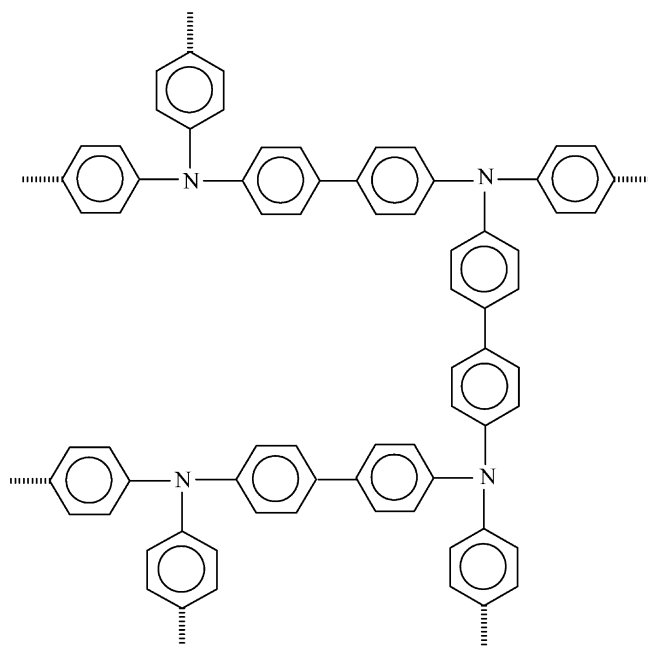
Keywords Poly(triphenylamine) · FTIR external reflection spectroscopy · Raman spectroscopy

Introduction

Only a few studies on fully conjugated three-dimensional systems have been reported, although research on macromolecules has grown dramatically during the last decade [1]. Special interest has been paid to the synthesis of oligomeric and polymeric materials based on triphenylamines, owing to their excellent hole transport capacity and possible use in organic electroluminescent devices [2, 3]. Low molecular weight polyamine materials have been synthesized and studied within the concept of mixed valence systems [4, 5]. Branched, conjugated poly(triphenylamine) (PTPA) has been chemically synthesized using different routes such as nickel-catalyzed dehalogenative polymerization [6] or the Grignard reaction of trihalogeno- or dihalogenotriphenylamine [7, 8]. Electrochemical synthesis provides fine control of the initiation and

termination steps during polymerization. This method also enables simultaneous in situ studies during the electrochemical process. Spectroscopic techniques such as Raman and FTIR are powerful when studying the dynamic changes taking place during the electrochemical charging and discharging of conjugated polymers.

In the present study, PTPA films have been electrochemically produced by oxidative polymerization of triphenylamine (Scheme 1). The dotted lines in the scheme mark the position for coupling of monomer units in the *para* position. Owing to the structure of the starting material, PTPA chains are not only limited to one-dimensional linear chains. The polymer structure is highly branched and, in addition to *para* coupling of the monomer units, *ortho* and *meta* coupling can take place. The electronic, structural and electrochemical properties have been studied by Raman, UV-vis and FTIR spectroscopy.



Scheme 1.

C. Kvarnström (✉) · P. Damlin · T. Lindfors · A. Ivaska
Process Chemistry Group,
c/o Laboratory of Analytical Chemistry,
Åbo Akademi University, 20500 Åbo-Turku, Finland
E-mail: ckvarnst@abo.fi

A. Petr · L. Dunsch
Group of Electrochemistry and Conducting Polymers,
Institute of Solid State Materials Research,
01107 Dresden, Germany

Experimental

Cyclic voltammetry

Electrochemical experiments were made in a three-electrode cell, using a platinum disk (7 mm^2) and platinum wire as the working electrode and counter electrode, respectively. A silver wire covered with chloride was used as a pseudo reference electrode, calibrated versus ferrocene. The electropolymerization medium was a mixture of acetonitrile (Lab-Scan, freshly distilled over CaH_2) and toluene (J.T. Baker) (1:4) containing 0.1 M of tetrabutylammonium hexafluorophosphate (TBAPF_6), TBAClO_4 or tetraoctylammonium tetrafluoroborate (TOABF_4) (all Fluka, electrochemical grade, dried under vacuum at 80°C before use; TBAClO_4 was dried at 40°C). Triphenylamine (Aldrich) was used as received. An EG&G Princeton Applied Research potentiostat/galvanostat (model 273) was used for the synthesis and characterization of the films. Prior to measurements the solution was purged with nitrogen, and all measurements were performed in a nitrogen atmosphere.

Raman spectroscopy

Raman spectra were recorded in situ in a spectroelectrochemical cell made for measurements at 90° through the microscope; see cell configuration in Fig. 1 [9]. The cell window was made of quartz. The working electrode was a Pt disk (7 mm^2), the counter electrode a Pt wire and the reference electrode a silver chloride-coated silver wire, calibrated versus ferrocene. Spectra were recorded at stepwise increased constant potentials. The laser was focused on the electrode on a spot of approximately $10 \mu\text{m}$ diameter through a $\times 30$ lens. The scattering was collected at 90° . The Raman spectrometer was a Renishaw Raman imaging microscope (system 1000 B) using a CCD detector. The laser excitation wavelength was $\lambda_{\text{exc}} = 780 \text{ nm}$. When using $\lambda_{\text{exc}} = 514.5 \text{ nm}$, Raman spectra were recorded in air from dry films on Pt substrates with a Jobin Yvon T 64000 spectrometer. Scattering was collected at 180° .

In situ FTIR spectroscopy

The in situ external reflection measurements were made in a spectroelectrochemical cell. The working electrode was a Pt disk (0.63 cm^2), while a Pt net around the working electrode served as the counter electrode. The reference electrode was a $\text{Ag}/\text{AgCl}/\text{Cl}^-$

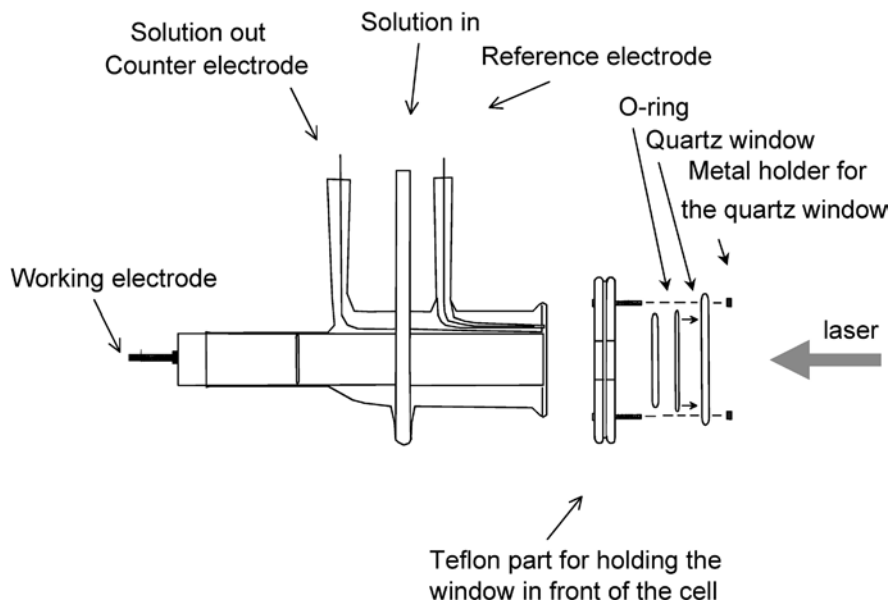
(3 M) electrode fitted with a glass bridge filled with electrolyte solution connected to a Luggin capillary placed close to the working electrode. The spectroelectrochemical cell is shown in Fig. 2. The potential at the working electrode was stepwise increased or decreased to charge or discharge the film and kept constant during recording of the spectra. Withdrawing the electrode from the window between measurements refreshed the thin electrolyte layer between the Pt disk electrode and the ZnSe window. FTIR spectra were recorded by a Bruker IFS66S spectrometer with a MCT detector. For each spectrum, 100 interferograms with a resolution of 4 cm^{-1} were coadded. In order to obtain specific spectral changes during an electrochemical process, a reference spectrum was taken at a potential where the studied electrode reaction does not take place. All the spectra shown here are difference absorption spectra.

Results and discussion

Cyclic voltammetry

PTPA films are made by potential scanning between 0 and 1.4 V at 50 mV/s in a mixture of toluene and acetonitrile (4:1) containing 0.1 M electrolyte salt and 0.05 M monomer [10]. The solvent mixture was used in order to obtain a polymerization medium with as low polarity as possible. In nonpolar solvents the solubility of the TPA cation and the formed dimer are decreased, which enables the precipitation of the formed oligomeric cations at the electrode. The cyclic voltammetric (CV) response of PTPA films prepared in the presence of different electrolytes (TBAPF_6 , TBAClO_4 and TOAClO_4) and cycled in monomer-free 0.1 M solution of these salts in acetonitrile is shown in Fig. 3a (second cycle of a freshly made film is shown). The scan rate in these experiments was 50 mV/s. The CV response from the film made and cycled in the presence of TOAClO_4 consists of a high oxidation current followed during the reverse scan by a small reduction. The film synthesized and cycled in the presence of TBAClO_4 shows a more reversible CV response than for the TOAClO_4 film and

Fig. 1. Spectroelectrochemical cell for in situ Raman measurements at 90°



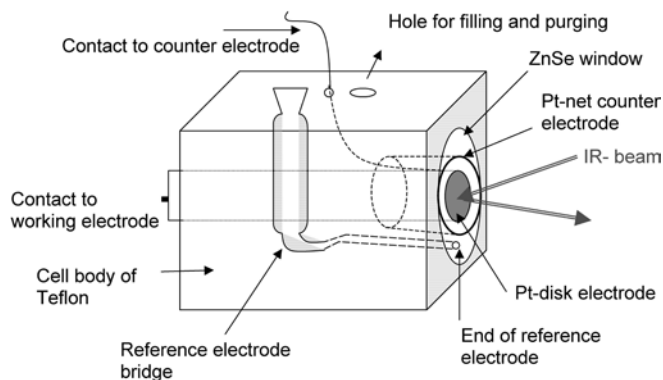
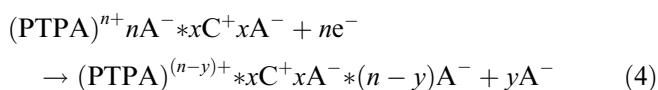
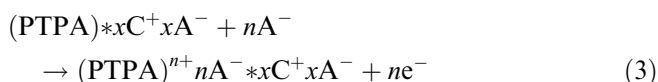
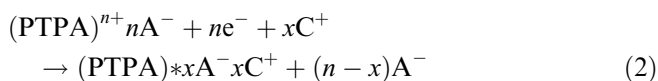
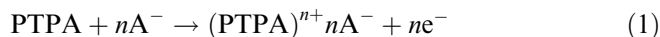


Fig. 2. Spectroelectrochemical cell for in situ external reflection FTIR measurements

the oxidation takes place at a lower potential. These differences in the CV response could be due to the size and mobility of the electrolyte cation.

Generally, the oxidation of conducting polymers is accompanied by insertion of electrolyte anions into the film followed by ejection of the inserted anions to the electrolyte solution upon reduction, as shown in Eq. 1:

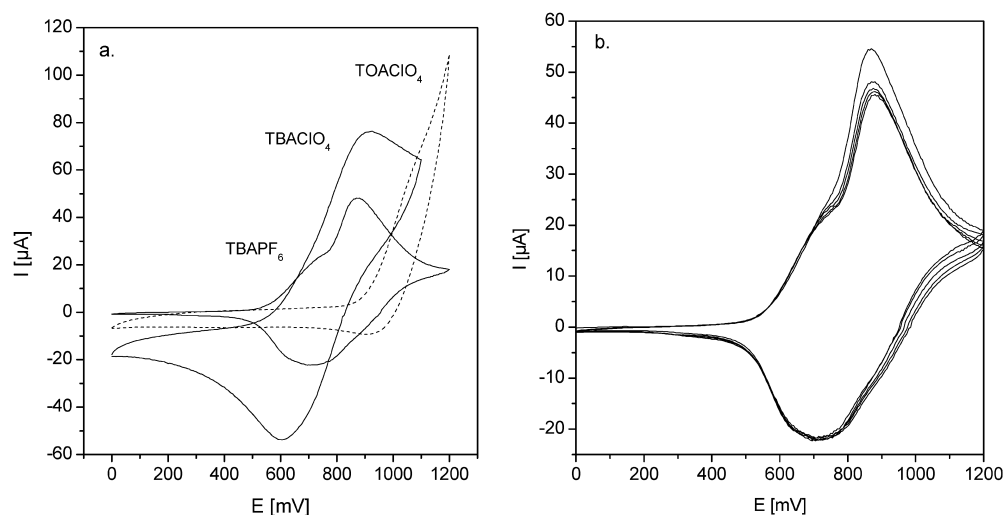


Equations 1, 2, 3, 4 are simplified descriptions of the actual processes. A^- is the dopant anion which compensates positive charges generated in the oxidized film.

The insertion and expulsion of anions has been shown to be not completely reversible [11, 12]. Inserted anions do not leave the film easily and cations (C^+) therefore have to act as charge compensators for the anions that are trapped deep inside the film and which are not removed during reduction (Eq. 2) [13, 14]. When polymerization is performed in the presence of a salt with large ions, the latter partly become immobilized in the polymer matrix and their diffusion between the film and the electrolyte during charging-discharging processes will be hindered owing to their size [15]. In the case that the cation is immobile and the neutral polymer film contains the salt C^+A^- and the polymer is electrochemically oxidized, the potential charge introduced in the film has to be balanced by diffusion of anions from the electrolyte according to Eq. 3. During the reduction of such a film, some of the anions move out of the film, while the concentration of cations inside the film remains unchanged owing to their low mobility and large size according to Eq. 4 when $y < n$. This might delay the reduction of the film and therefore just a small reduction current can be recorded during the reverse scan. Evidence that the material is not completely reduced can be seen in the Raman and FTIR spectra shown later in this paper.

As can be seen in Fig. 3a, the films formed and cycled in the presence of TBAPF_6 show almost reversible redox behavior. Two overlapping oxidation peaks can be observed, with the main oxidation peak at 850 mV. A broad reduction peak at 700 mV is obtained during the reverse scan. The charge involved in the doping process is slightly lower than for films made and cycled in the presence of TBAClO_4 . The most stable response from switching between the neutral and conductive state, however, was obtained with the film made in TBAPF_6 . This film can also be cycled repetitively several times without any significant change in the CV response (Fig. 3b). Even after storage of the dry film in room atmosphere for several days the original CV could be regained. The color of the film changes from transparent when neutral to bright blue upon oxidation.

Fig. 3. **a** Cyclic voltammograms of PTPA films synthesized and cycled in three different electrolytes. Scan rate 100 mV/s; second cycle of a freshly made film. **b** First five cycles of a PTPA film in 0.1 M TBAPF_6 . Scan rate 100 mV/s



Raman spectroscopy

The Raman spectra of a dry PTPA film electropolymerized in 0.1 M TBAPF₆ and measured with two different excitation lines, $\lambda_{\text{exc}} = 514.5$ nm and $\lambda_{\text{exc}} = 780$ nm, are shown in Fig. 4. As seen in the figure, the Raman spectrum of PTPA is very sensitive to the excitation wavelength. A similar influence of the excitation line on the Raman spectra of polyaniline (PANI) has also been reported in the literature [16]. The obvious reason for the different spectra at these two excitation wavelengths is that the chemical structure of PTPA consists either of quinoid or benzenoid units, as found in PANI, or a combination of both of them, depending on

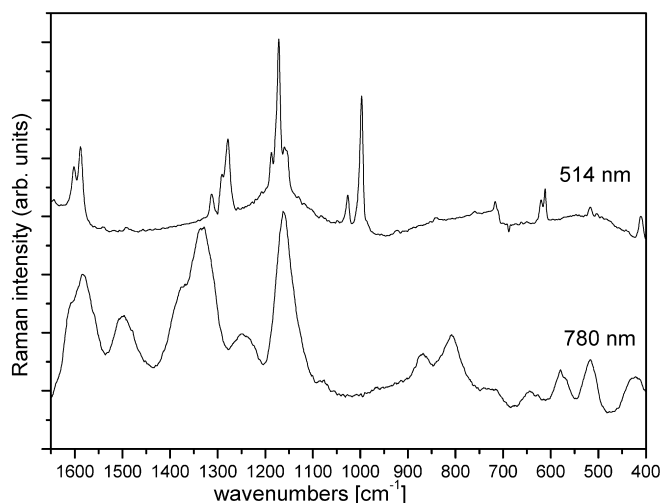


Fig. 4. Raman spectra of a PTPA film electropolymerized in 0.1 M TBAPF₆ measured with $\lambda_{\text{exc}} = 514.5$ nm and $\lambda_{\text{exc}} = 780$ nm

the oxidation states of the polymer. Consequently, the vibrations originating from either quinoid or benzenoid units will be resonance enhanced differently by the applied excitation lines.

When the energy of the excitation line coincides with the optical absorption originating from the conjugated material in a certain state, the Raman modes associated with the segments in the polymer giving rise to the said optical absorption will be enhanced.

The Raman spectrum of PTPA ($\lambda_{\text{exc}} = 514.5$ nm) resembles the spectrum of *N,N'*-1,4-phenylenediamine, which is a lower derivative of the fully reduced leucoemeraldine base form of PANI [17, 18]. According to the reported assignments for the Raman bands of *N,N'*-1,4-phenylenediamine, the following assignment of the bands in Fig. 4 ($\lambda_{\text{exc}} = 514.5$ nm) can be made. The Raman bands at 611, 998 and 1028 cm^{-1} are assigned to ring deformations of the benzenoid ring [19]. The bands at 1150, 1170 and 1185 cm^{-1} originate from C-H bending and the bands at 1277 and 1290 cm^{-1} are due to C-N antisymmetric stretching and C-H bending. The Raman band at 1320 cm^{-1} originates from C-H bending of the benzenoid ring. The bands observed at 1588 and 1610 cm^{-1} are from C-C ring stretching. Raman bands characteristic of monosubstituted benzene at 998 and 1028 cm^{-1} are present in the spectra owing to the network structure of PTPA (Scheme 1) [18]. The Raman bands measured at $\lambda_{\text{exc}} = 514.5$ nm are listed in Table 1. Additionally, proposed assignments reported in the literature on PANI-type material are also given.

Excitation lines in the red or IR region favor the excitation of oxidized units in the polymer. Consequently, bands originating from the quinoid units will be resonance enhanced in the Raman spectra. Comparing the spectrum obtained with $\lambda_{\text{exc}} = 780$ nm in Fig. 5 with

Table 1. Raman bands obtained with $\lambda_{\text{exc}} = 515.5$ nm and $\lambda_{\text{exc}} = 780$ nm from a dry PTPA film made potentiodynamically in the presence of TBAPF₆

Dry film (515.5 nm)	Dry film (780 nm)	Neutral film (400 mV)	Charged film (1300 mV)	Assignment ^a	Ref
611	640	—	—	Ring deformation (B)	[17, 22]
—	—	740	—	Imine deformation	[22]
—	810	820	—	Ring stretching	[21]
—	870	—	—	Ring deformation	[20, 22]
998	—	—	—	C-H out-of-plane wag, monosubst. benzene	[19]
1028	—	—	—	Ring deformation (B), monosubst. benzene	
1150	—	—	—	C-H in-plane bending	
—	1165	1167	1164	C-H in-plane bending (Q)	[16, 22]
1170	—	—	1181	C-H in-plane bending from benzenoid rings	[16]
—	1248	—	—	C-N stretching (Q)	[16]
1277	—	1285	1288	C-N stretching (B)	[16]
1290	—	—	—	C-H bending	[17]
1320	1335	—	1339	C-N stretching	[17]
—	1375	—	1375	C-N stretching	[21, 25]
—	—	1446	1481	C-N stretching (Q)	[16, 17, 22]
—	1501	—	1522	C-C and C=C stretching (Q)	[16]
—	—	—	1569	C=C stretching (Q)	[16, 22]
1587	1585	1598	1582	C-C stretching (Q)	[16]
1610	1615	1607	—	C-C stretching (B)	[16]

^aB = benzenoid; Q = quinoid

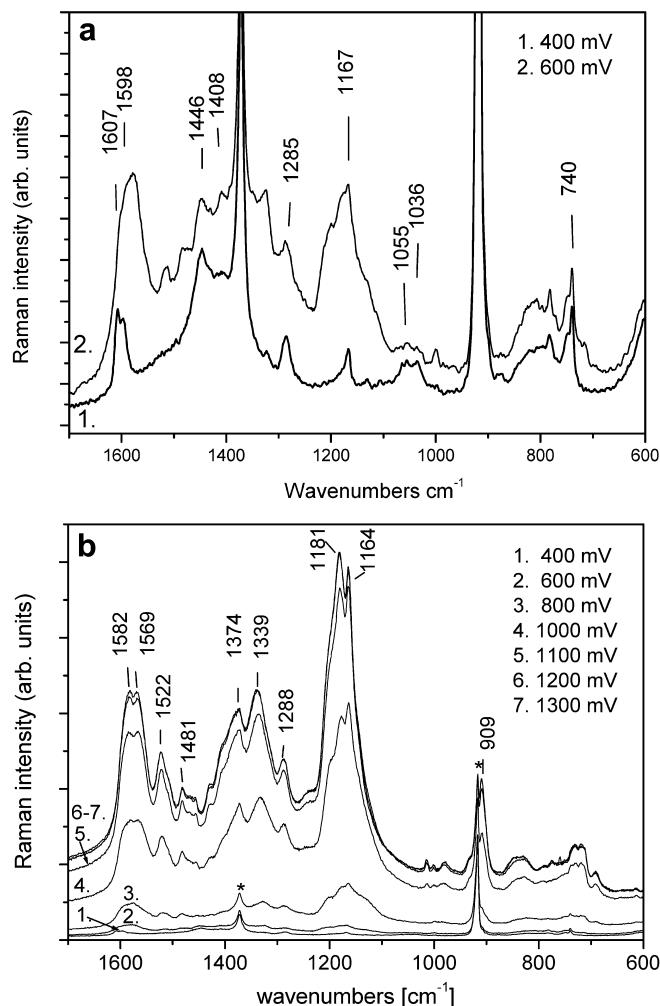


Fig. 5a, b. In situ Raman spectra of a PTPA film on a Pt electrode in 0.1 M TBAPF₆-acetonitrile. **a** The first two spectra of the beginning of the doping. **b** The Raman spectra recorded at constant potential during charging (p-doping)

spectra reported for PANI [16, 20] obtained with $\lambda_{\text{exc}} = 676.4$ or 780 nm, the following assignments are valid also for PTPA. The band at 810 cm^{-1} has been assigned to symmetric ring stretching [21] and that at 870 cm^{-1} to in-plane ring deformation [22, 23]. A band from C-H in-plane bending and deformation of quinoid-type rings can be seen at 1165 cm^{-1} [22]. The band at 1248 cm^{-1} has been associated with the C-N stretching mode [16, 24]. Bands in the $1300\text{--}1350 \text{ cm}^{-1}$ region, also from C-N stretching, have in PANI been associated with protonation. In poly(*N*-methylaniline) a shift of the band from C-N stretching to 1374 cm^{-1} due to direct substitution at the nitrogen atom was observed [25]. This band has also been associated with cross-linking in PANI structures [26]. When PANI is equilibrated in solutions of different pH, a peak at 1375 cm^{-1} was obtained when measured with $\lambda_{\text{exc}} = 1064 \text{ nm}$ [27]. In the PTPA case, a band split is obtained with peaks at 1370 and 1335 cm^{-1} . At 1500 cm^{-1} a broad band is seen in PTPA. This spectral range can in principle contain many different modes, such as C-C and C=C stretching deformations of qui-

noid rings or a C=N stretching deformation. Bands similar to neutral PANI are also the overlapping bands at 1582 and 1605 cm^{-1} . The peak at 1582 cm^{-1} is assigned to a C=C stretching deformation in the quinoid ring and the second one to a C-C stretching deformation in a benzenoid-type ring. In PANI it was noticed that upon doping these peaks were shifted to 1587 and 1620 cm^{-1} , respectively [16]. The bands obtained with $\lambda_{\text{exc}} = 780 \text{ nm}$ are also included in Table 1.

Owing to the presence of the Raman band at 1335 cm^{-1} it is evident that quinoid structures are present in the PTPA film. It should be noted that the PTPA electrode was cycled in the potential region $0\text{--}1200 \text{ mV}$ (in TBAPF₆) prior to the Raman measurements. The cycling was stopped at 0 mV and the PTPA film was then allowed to dry before measurements. Consequently, the PTPA film should then be in the neutral form. The presence of quinoid structures in the neutral film may be due to excitation of the sample by the laser ($\lambda_{\text{exc}} = 780 \text{ nm}$).

The influence of doping of the PTPA film on the Raman spectra was further studied by in situ measurements of the film. After film preparation the electrode was moved to the spectroelectrochemical cell containing 0.1 M TBAPF_6 in acetonitrile. In Fig. 5 the Raman spectra taken at different applied potentials are shown. Figure 5a shows the spectral changes from the neutral state to a slightly doped state. The most distinct changes take place in the region between 1600 and 1300 cm^{-1} . The strongest vibration in this region is due to C-C and C=C stretching from the quinoid rings at 1598 cm^{-1} that shifts to 1582 cm^{-1} upon doping. New peaks can be seen at 1500 and 1446 cm^{-1} from C=C and C=N stretching, respectively. These two bands shift towards higher wavenumber upon further doping. At low doping levels, bands from the solvent strongly interfere with the spectrum of the polymer in this wavenumber region. Figure 5b shows the spectral changes that take place during further doping. In addition to the above-mentioned changes, two new peaks at 1375 and 1335 cm^{-1} , assigned to C-N stretching (cationic), appear [21]. The final spectrum obtained at a high doping level is similar to the one obtained from the slightly photoexcited dry film measured at 780 nm . The spectrum of the electrochemically doped form is slightly more resolved, probably owing to a more stable excited state of the polymer during the recording of the spectrum.

FTIR spectroscopy

The FTIR spectrum taken ex situ by external reflection of a dry PTPA film, electrodeposited on a Pt sheet, is shown in Fig. 6. Vibrations from C-C ring stretching at 1550 cm^{-1} , from C-C stretching and C-H bending at 1491 cm^{-1} and from C-H bending at 1321 and 1154 cm^{-1} can be observed in the spectrum [17, 28]. The band at 1274 cm^{-1} has been assigned to C-N stretching, from tertiary amines [3, 28, 29]. At 1000 cm^{-1} a peak from

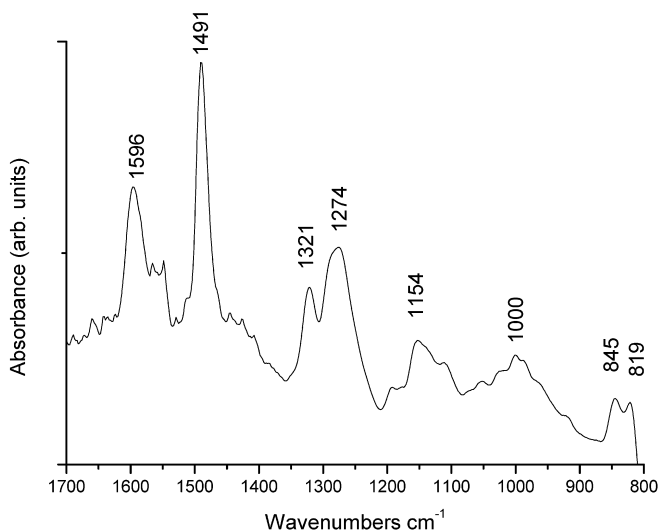


Fig. 6. FTIR spectrum taken from a dry PTPA film by total reflection. The film was made in 0.1 M TBAPF₆-toluene-acetonitrile solution

ring deformation is seen, and the vibration at 845 cm⁻¹ results from both ring deformation and C-H out-of-plane vibration [28]. The band at 819 cm⁻¹ is assigned to a C-H out-of-plane vibration from 1,4-disubstituted benzene rings [3]. The presence of bands at 1274 and 819 cm⁻¹ indicates coupling of the starting material, i.e. that C-C bonding between the benzene rings of the triphenylamine units has taken place. The spectrum also contains bands from quinoid sections of the film. Vibrations from C=C stretching at 1596 cm⁻¹ and from C-H bending at 1109 cm⁻¹ can also be associated with the quinoid structures. In Table 2 the main IR vibrations are listed, together with the proposed assignments reported in the literature for PANI-type materials. The presence of quinoid parts in the spectrum indicates that the polymer is not fully discharged, although the electropolymerization process performed by potential

Table 2. Infrared vibrations of a dry PTPA film made potentiodynamically in the presence of TBAPF₆. Proposed assignments are given according to the literature

Frequency (cm ⁻¹)	Assignment ^a	Ref
819	C-H out-of-plane vibration from <i>para</i> -disubstituted benzene rings	[3, 29]
845	C-H out-of-plane vibration + ring deformation	[28]
1000	Ring deformation	[28]
1109	C-H bending (Q)	[28]
1154	C-H bending (B)	[28]
1274	C-N stretching from tertiary amines	[3, 28, 29]
1321	C-H bending (B)	[28]
1491	C-C stretching and C-H bending (B)	[17, 28]
1550	C-C ring stretching (B)	[28]
1596	C-C stretching (Q)	[17, 28]

^aB = benzenoid; Q = quinoid

cycling was stopped at 0 V where the polymer should be in the reduced form. The presence of some quinoid parts is probably due to a slight separation of the charge carriers caused by the highly crosslinked structure of the polymer.

Upon charging of conjugated materials, new bands appear in the IR spectrum from 1500 to 700 cm⁻¹, typically termed the IR-active vibration bands (IRAV). These bands are usually 20–30 times stronger in intensity than the corresponding bands from pristine materials. The intensity of the IRAV bands grows linearly with increasing concentration of charge carriers in the film [30]. The doping-induced IRAV bands are generally independent of the doping species. Attempts to explain the characteristics of the charge carriers consistent with the IR observations were first made by Horovitz and co-workers [31] for *trans*-polyacetylene by introducing the “pinning parameter”, which is used as a measure of the localization of “defects”. In this theory, Horovitz combines the charge density wave with the fact that p-electrons are coupled to the motion of the polymer backbone. Zerbi and co-workers [32] introduced the “effective conjugation coordinate, ECC” as a starting point for the understanding of doping-induced spectral changes in conjugated systems. This coordinate represents the dynamic changes between the two limiting structures (benzenoid and quinoid) reached upon charging and discharging of the polymer.

In order to study whether electrochemical charging-discharging processes cause similar doping-induced spectral changes in PTPA, FTIR difference spectra have been recorded during p-doping and are shown in Fig. 7. The CV response from films prepared and cycled in the FTIR cell is shifted by approx. 240 mV to higher potentials relative to films made and measured in a conventional electrochemical cell (Fig. 2). The potential shift is partly due to the different cell geometry in the in situ cell and partly due to the greater film thickness in the FTIR cell. The reference spectrum used in Fig. 7 is recorded at 840 mV, where the Faradaic current starts to increase during p-doping. In the region 1700–700 cm⁻¹ of the spectra shown in Fig. 7a (enlarged in Fig. 7b), doping-induced IRAV bands grow in intensity with increasing applied potential at 1610, 1570/1580, 1477, 1370/1345, 1305, 1255 and 1190/1170 cm⁻¹. The large intensity, which is usual for IRAV bands, is explained by the large charge flux along the carbon-carbon bonds induced by the ECC, which generates a large variation in the molecular dipole moment directed along the chain axes. Parallel to the evolution of IRAV spectra during doping is an increase in the electronic absorption with increasing doping level observed at low energies. This broad absorption starting from 2000 cm⁻¹ is associated with the formation of charge carriers and is typical for conducting polymers [33].

The spectra in Fig. 7 are difference spectra and therefore some downward pointing bands indicate a loss of certain structures when the material is doped. The negative band at 1496 cm⁻¹ from ring vibration from

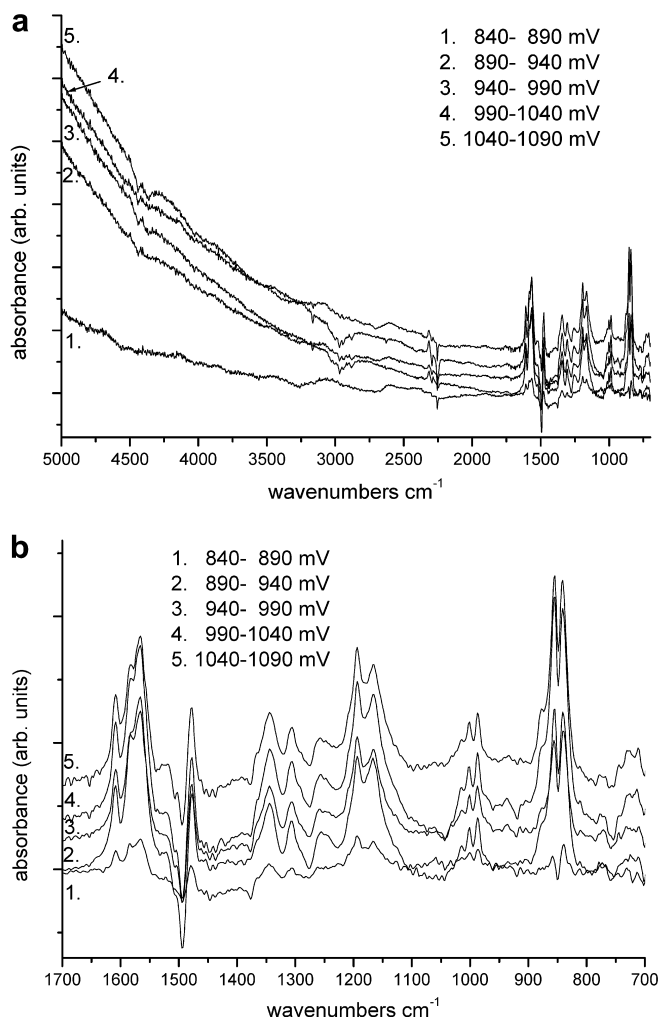


Fig. 7. **a** In situ difference external reflection FTIR spectra of the p-doping of a PTPA film in 0.1 M TBAPF₆-acetonitrile solution. Spectra were gathered at constant potentials every 50 mV. Reference spectrum was taken at 840 mV. Sequence: *bottom to top*. **b** Enlargement of the region containing the IRAV bands at 1700–700 cm⁻¹ of the spectra shown in **a**

benzenoid rings can be considered to be due to a decrease in the amount of benzenoid structures in the doped material. Owing to the nature of IRAV bands, an exact interpretation of every band is difficult. Bands at 1477 and 1570 cm⁻¹, however, can be assigned to semiquinoid structures, also reported for PANI [34].

Conclusions

Electrochemical synthesis of triphenylamine leads to the network structure of a conjugated polymer. The film can be positively charged and discharged, resulting in structural changes between benzenoid and quinoid rings. The polymer film consists of both benzenoid and quinoid units, suggesting that even after discharging some trapped charge carriers remain in the polymer. The IR spectral pattern from the charged polymer shows, for the

most part, an enhancement of bands already present in the “neutral form” but slightly shifted in wavenumber. Raman spectra of a dry film in air also reveal the presence of the quinoid ring structure. Under potential control (0 V), some of the bands from the quinoid structure disappear, but, as in IR, evidence of trapped segments of “semiquinoid” structures can be found. The IR spectrum of charged (doped) film is similar to the Raman spectrum of the neutral (undoped) film, indicating that the charge carriers (electrons) break the structural symmetry in the polymer and therefore make otherwise silent IR modes active.

Acknowledgements The authors gratefully acknowledge financial support for this research from the Deutsche Akademische Austauschdienst and the Academy of Finland and Graduate School of Materials Research, Åbo Akademi University (P.Damlin). This work is a part of the Åbo Akademi University, Process Chemistry Group, within the Finnish Centre of Excellence Programme (2000–2005). Tech. Lic. Paul Ek is gratefully acknowledged for the Raman cell construction.

References

1. Tour JM (1996) *Chem Rev* 96:537
2. Kuwabara Y, Ogawa H, Inada H, Noma N, Shirota Y (1994) *Adv Mater* 6:677
3. Tanaka S, Takeuchi K, Asai M, Iso T, Ueda M (2001) *Synth Met* 119:139
4. Bonvoisin J, Launay J-P, Verbouwe W, Van der Auweraer M, De Schryver FC (1996) *J Phys Chem* 100:17079
5. Lambert C, Nöll G (1998) *Angew Chem Int Ed* 37:2107
6. Yamamoto T, Hayashi Y, Yamamoto A (1978) *Bull Chem Soc Jpn* 51:2091
7. Ishikawa M, Kawai M, Ohsawa Y (1991) *Synth Met* 40:231
8. Tanaka S, Iso T, Doke Y (1997) *Chem Commun* 2063
9. Damlin P, Kvarnström C, Petr A, Ek P, Dunsch L, Ivaska A (2002) *J Solid State Electrochem* (in press)
10. Petr A, Kvarnström C, Dunsch L, Ivaska A (2000) *Synth Met* 108:245
11. Lim JY, Paik W, Yeo I (1995) *Synth Met* 69:451
12. Bruckenstein S, Brzezinska K, Hillman RA (2000) *Electrochim Acta* 45:3801
13. Naoi K, Lien M, Smyrl WH (1991) *J Electrochem Soc* 138:440
14. Xie Q, Kuwabata S, Yoneyama H (1997) *J Electroanal Chem* 420:219
15. Carlier V, Skompska M, Buess-Herman C (1998) *J Electroanal Chem* 456:139
16. Quillard S, Berrada K, Louarn G, Lefrant S, Lapkowski M, Pron A (1995) *New J Chem* 19:365
17. Quillard S, Louarn G, Lefrant S, MacDiarmid AG (1994) *Phys Rev B* 50:12496
18. Quillard S, Louarn G, Buisson JP, Lefrant S, Masters J, MacDiarmid AG (1992) *Synth Met* 49–50:525
19. Cochet M, Quillard S, Buisson JP, Lefrant S, Louarn G (1999) *Synth Met* 101:793
20. Lindfors T, Kvarnström C, Ivaska A (2002) *J Electroanal Chem* 518:131
21. Furukawa Y, Ueda F, Hyodo Y, Harada I, Nakajima T, Kawagoe T (1988) *Macromolecules* 21:1297
22. Berrada K, Quillard S, Louarn G, Lefrant S (1995) *Synth Met* 69:201
23. Quillard S, Louarn G, Buisson JP, Lefrant S, Masters J, MacDiarmid AG (1993) *Synth Met* 55:475
24. Laska J, Girault R, Quillard S, Louarn G, Prón A, Lefrant S (1995) *Synth Met* 75:69
25. Kilmartin P, Wright G (1999) *Synth Met* 104:145

26. da Silva JEP, de Faria DLA, Córdoba de Torresi SI, Temperini MLA (2000) *Macromolecules* 33:3077
27. Englert C, Umapathy S, Kiefer W, Hiro-o-hamaguchi (1994) *Chem Phys Lett* 218:87
28. Boyer MI, Quillard S, Rebourt E, Louarn G, Buisson JP, Monkman A, Lefrant S (1998) *J Phys Chem B* 102:7382
29. Tanaka S, Takeuchi K, Asai M, Iso T, Ueda M (2000) *Mater Res Soc Symp Proc* 600:179
30. Del Zoppo M, Castiglioni C, Zuliani P, Zerbi G (1998) In: Skotheim TA, Elsenbaumer RL, Reynolds JR (eds) *Handbook of conducting polymers*. Dekker, New York, p 765
31. Ehrenfreund E, Vardeny Z, Brafman O, Horovitz B (1987) *Phys Rev B* 36:1535
32. Castiglioni C, Gussoni M, Lopez-Navarrete JT, Zerbi G (1988) *Solid State Commun* 65:625
33. Kuzmany H, Sariciftci NS, Neugebauer H, Neckel A (1988) *Phys Rev Lett* 60:212
34. Ping Z, Neugebauer H, Neckel A (1996) *Electrochim Acta* 41:767